JOURNAL OF MATERIALS SCIENCE 31 (1996) 1803–1808

An experimental micromechanics measurement technique for submicrometre domains

C. R. CORLETO
Department of Mechanical and Industrial Engineering, Texas A&M University at Kingsville, Kingsville, TX 78 363, USA

W. L. BRADLEY
Department of Mechanical Engineering, Texas A&M University, College Station, TX 77 843, USA

H. F. BRINSON
Department of Mechanical Engineering, University of Houston, Houston, TX 77 204, USA

Orthogonal arrays of dots applied to surfaces can be used to directly measure microscopic strain fields. The spatial and strain resolution are both limited by the size of the dots placed on the surface. Two techniques using the beam of a scanning electron microscope (SEM) have been developed which make possible the placement of very fine dots with diameters of only 0.5 and 0.02 μm, respectively, on the surface of the specimen, allowing local strain measurements on the scale of 0.2–10 μm when specimens are loaded in the SEM. Measurements of strains fields around the tips of growing cracks in both polymers and polymeric composites are presented to illustrate the capabilities of the technique.

1. Introduction

Attempts to understand macroscopic mechanical properties, especially ductility and fracture toughness, require a more detailed understanding of material behaviour on a microscopic scale, which with current technology it should be possible to measure directly. New techniques are now being developed which have as their goal determination of strain fields on a scale of micrometres. Mao *et al.* [1] reported a technique for determining the strain field at a crack tip using a photoresist layer which deformed with the specimen. Brown and Wang [2] measured the strain distribution in the neighbourhood of a craze, with a method in which the change in the spacing of razor blade scratches was measured as a function of position. Hibbs and Bradley [3] measured strain fields directly using dot maps created by an electron beam in a scanning electron microscope. Davidson and Lankford [4] used selected area electron channelling and stereo-imaging to determine strain distributions at crack tips. James *et al.* [5] developed a new system based on digital image cross-correlation for measuring surface displacement fields. More recently, Dally and Read [6] have developed a technique using the electron beam scanner in an SEM to both place the initial series of lines and then develop a moiré pattern when the specimen (and surface grid) are deformed, extending optical techniques for micromoiré developed by Post [7]. Proceedings of an American Society for Mechanical Engineers Symposium held in 1989 and edited by W. N. Sharpe Jr summarizes much of the development work in this area to date [8].

The present work is based on the method developed by Hibbs and Bradley [3], but with considerable refinement. In particular, a new technique has been developed which allows the placement of 20 nm diameter dots on the surface of a specimen to use as displacement markers, allowing the relative displacement between these dots to be determined when the specimen is loaded in the SEM. The very small size of these dots allows local strains on the scale of 0.1–0.2 μm to be measured.

In this paper the theoretical relationship between dot size, spatial resolution and strain resolution will be discussed, leading to the conclusion that very fine dots are essential for high spatial and strain resolution work. Then two techniques for applying very fine dots using the electron beam in an SEM will be described with experimental results presented. Finally, the utility of the technique will be illustrated by presenting strain field maps around the tips of growing cracks in several different material systems.

1.1 Theoretical considerations in spatial and strain resolution

An orthogonal array of dots such as used in this work is presented in Fig. 1a schematically, with an actual array as generated in the SEM in Fig. 1b. Assume for purposes of discussion that a high resolution image analyser for the SEM will have 1000 pixels in the horizontal and vertical directions for an image projected on a 100 × 100 mm view screen, off of which digital information may be collected. The actual dimensions

0022–2461

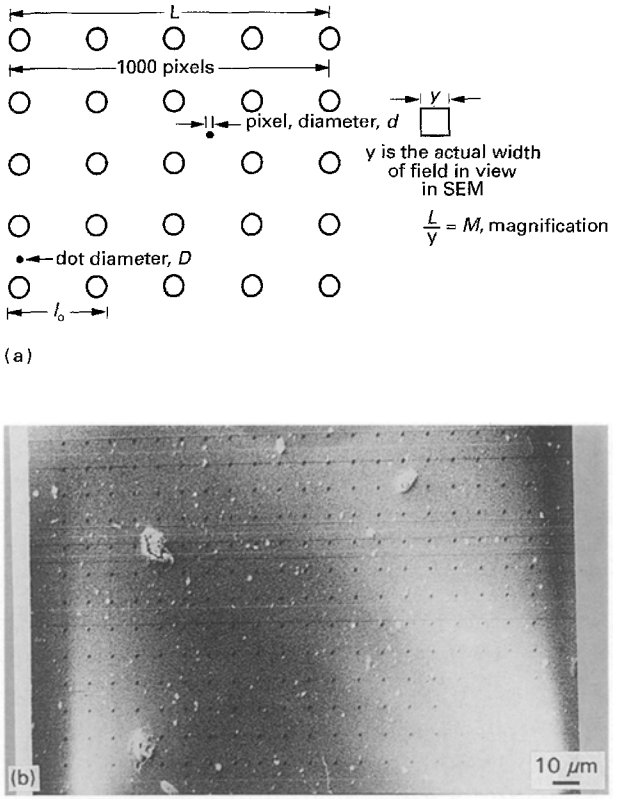

Figure 1 (a) Schematic of orthogonal grid of dots where the pixel diameter corresponds to an actual distance of $d = L/(M \times n)$ on the specimen being viewed (where $n = 1000$ is assumed for purposes of illustration and the pixel diameter is not drawn to scale). Pixel diameter represents the limit of resolution for image analysis. The number of pixels in commercial systems is usually either 512 or 1024. (b) Actual specimen of rubber toughened epoxy with dot map placed near the crack tip of a compact tension specimen (far left, midway up the photograph).

of the portion of the specimen in view is of course determined by the screen size divided by the magnification. For example, at × 1000 an area of 0.1 × 0.1 mm is in view. Furthermore, each pixel corresponds to a square of 0.1 × 0.1 μm. From this discussion, it is clear that the physical dimension on the specimen represented by each pixel in the image analyser is given by

$$d = L/(M \times n) \tag{1}$$

where d is the actual dimension on the specimen being observed, corresponding to one pixel in the image analyser; L is the actual dimension of the image generated by the SEM; M is the operating magnification of the SEM; and n is the number of pixels in the same direction as L, as seen in Fig. 1a.

The relationship between dot size, spatial resolution and strain resolution will be considered next. First, consider a system in which the dot size corresponds to the pixel size. For the example presented above, this would mean dots with 0.1 μm diameters. If the spacing between dots used to measure the strain was maximized, the effective gauge section would be 1000 pixels, with a minimum measurement of change in length of 1 pixel, giving a strain resolution of 0.001, or 0.1%.

It is clear from this illustration that the relative size of the dots to the distance between dots determines the strain resolution. If a better spatial resolution for the strain measurement is desired, then a distance of only 100 pixels between dots might be used (10 μm in the previous example), giving a strain resolution of 1/100, or 1%. Thus, it is clear that greater strain resolution is only obtained at the expense of spatial resolution and visa versa. As long as the dot diameter corresponds to one pixel, the smallest strain change that can be resolved between adjacent dots, $\Delta\varepsilon$, is given by

$$\Delta\varepsilon = d/l_0 \tag{2}$$

where d is the pixel diameter, and therefore, the dot diameter, as per the assumption at this time; l_0 is the distance between dots, which is the smallest effective local gauge length over which the strain is being measured, as seen in Fig. 1a. If the effective gauge length is given by the number of pixels between two specific dots on the surface times the pixel diameter, $m \times d$, then Equation 2 for limiting strain simplifies to

$$\Delta\varepsilon = d/m \times d = l/m \tag{3}$$

for the case in which the actual dot diameter corresponds to one pixel in the SEM image, which is obviously a rather special case. A similar relationship was obtained by Dally and Read [6] for electron beam moiré, where their m corresponded to the number of lines etched between two points which defined the effective gauge length for their strain measurement.

The situation becomes a bit more complicated when the dot size is larger than one pixel, as it is generally found to be in practice. Standard image analysis techniques may be used to determine the centre of the dot, making the uncertainty in the dot location somewhat less than the dot diameter, which was previously used when the dot size corresponded to one pixel in Equation 2.

If the dot diameter, D, is equal to $w \times d$ and if the uncertainty in dot centre is given by some fraction, f, of the number of pixels (which decreases as the dot size increases, but more slowly than an inverse relationship), then the uncertainty in the strain measurement originally given in Equation 2 (for case where the pixel diameter equal to dot diameter) becomes

$$\Delta\varepsilon = D \times f/l_0 = w \times d \times f/m \times d = w \times f/m \tag{4}$$

Equation 4 implies that the ratio of the number of pixels in the dot to the number of pixels in the effective gauge length determines the strain resolution, with the caveat that $f = f(w)$, and decreases as the number of pixels needed to transverse the dot diameter increases.

On first glance, it would appear that strain resolution is independent of the magnification used in the SEM, since w/m remains constant as one increases magnification, assuming the length remains the distance between two adjacent dots. However, since f decreases with increasing w, and w increases with increasing magnification (since $w = D/d$ and d decreases with increasing magnification, as seen in Equation 1), strain resolution is indeed enhanced at higher magnification.

In summary, it is seen that strain resolution is determined by the ratio of the number of pixels required to transverse a dot to the number of pixels in the gauge section. This clearly implies

1. that higher strain resolution for a given gauge section or
2. a smaller allowable gauge section (higher spatial resolution) for a given strain resolution

is made possible by using the smallest dots one can produce on the surface. A more desirable combination of strain and spatial resolution is achievable at higher magnifications through the f factor in Equation 4, though the effort to map a larger strain field goes up substantially at higher magnifications. This analysis suggests that measurement of displacement and strain fields on a microstructural level requires the use of very fine dots (or lines in the case of electron beam moiré). In the next section, two techniques to put very fine dots on the surface of a specimen will be described with actual experimental results presented.

2. Experimental procedures and results

Two techniques have been developed to apply very fine dots to the surface of specimens using the electron beam in the SEM.

2.1. Burning holes in the AuPd coating

The beam may be used to burn small holes in the 10 nm thick gold–palladium sputter coating applied to many specimens to minimize charging. The electron beam is used in spot mode in conjunction with a stage with x–y stepping motors which are computer controlled. The SEM magnification is set (typically about $\times$ 500–1000) and the condenser lens adjusted to give a spot of suitable size (typically about 0.5–1.0 μm). The burning of each hole takes only a few seconds (about 5 s was common in this work), allowing an orthogonal matrix of 100 holes to be burned in about 10 min. These dots will appear as dark spots on the specimen, as seen in Fig. 1b. The loading of this same specimen, which is a rubber toughened epoxy, and the consequent distortion of the dot map is seen in Fig. 2.

The highest spatial resolution is obtained by measuring the change in distance between adjacent dots; however, this results in the lowest strain resolution. The ratio of dot size to spacing between dots is approximately 1/20, suggesting a strain resolution of 5% or less for this case of maximum spatial resolution (using the change in distance between two adjacent dots). The strain resolution can be enhanced by either changing the magnification of the photograph in the SEM to make each dot include more pixels [reducing $f(w)$ in Equation 4] or else the photograph itself can be enlarged using a Xerox machine from a 75×100 mm to a 225×300 mm size, allowing a more precise measurement of the translation of the dot centres using the digitizing board or a digital caliper. This technique allowed the uncertainty in the measured strain to be reduced to $\pm$ 1.5%, as determined by multiple measurement made by several different persons in this study.

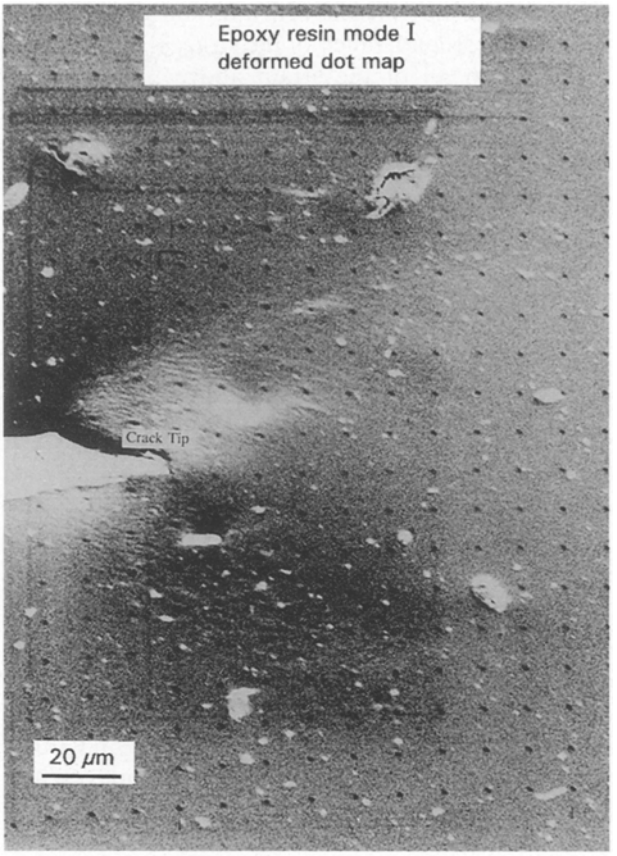

Figure 2 Distorted dot map at tip of crack in compact tension specimen loaded to a level just below that required for crack growth; compare to Fig. 1b before loading.

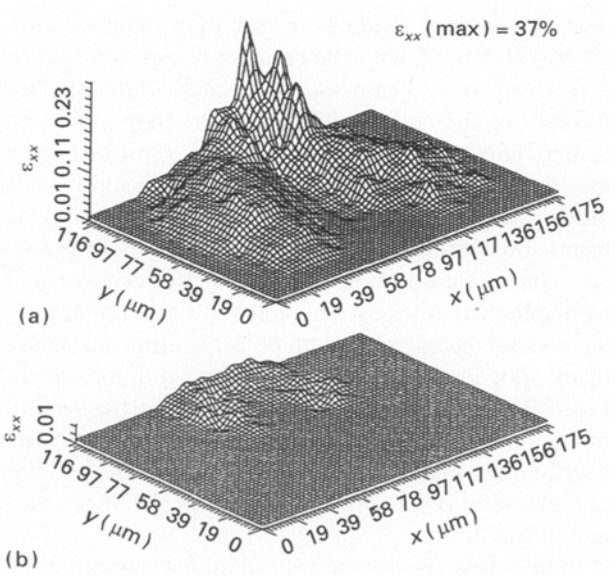

Figure 3 Strain field map for (a) compact tension specimen loaded in the x-direction to a level just below that required to cause crack growth, with crack tip $x = 88$, $y = 116$, $\varepsilon_{xx}(\max) = 37\%$ determined using Fig. 1b and 2. (b) Same as Fig. 3a except after complete unloading.

The resultant strain field map is presented in Fig. 3a, b, which indicates the strain field at a load approaching that required to grow the crack and after unloading, respectively. There are two surprising results from the crack tip strain field map: first, the crack tip strain to failure is 37% for an epoxy whose

elongation in a tensile test with a 25 mm gauge section is only 5%; second, much of the strain is recoverable, even though all of the strain above 2% is highly non-linear. Clearly, elongation in rubber toughened epoxies is controlled more by incipient flaws than by intrinsic ductility. Subsequent annealing of this specimen removed even the residual strain indicated in Fig. 3b after unloading, indicating essentially all of the strain preceding fracture is viscoelastic, and, thus, fully recoverable.

The only limitation in this technique is that a beam of sufficient intensity to burn small holes must be used and this in turn limits the minimum size of the dots that can be produced to approximately 0.5 μm. To make finer yet dots, the technique described in the next section has been developed.

2.2. Raised dots

When the SEM is used at a high magnification for some extended period of time and then returned to a lower magnification, one can usually see a discolouration in the region previously rastered by the electron beam. This is sometimes called contamination writing and can potentially be used to make dots on the surface.

During both sputter coating of the gold–palladium and subsequently during observation in the SEM, the surface of the specimen becomes coated with contamination, consisting primarily of diffusion pump oil. This very thin coating of polymers has a relatively high coefficient of thermal expansion. If the SEM is operated in spot mode at a very high magnification ($\times$ 20 000–50 000) with the condenser lens adjusted to give a very small beam spot size, small white dots are formed on the surface. The fact that they are white rather than black indicates that they represent local raised spots on the surface. The electron beam in spot mode provides local heating of the area of the circular beam spot, resulting in thermal expansion of the surface contamination until instability produces a small hemispherical pucker. The pucker itself apparently has a small recess at its north pole, resulting in a small, black spot in the centre of the white dot, as seen in Fig. 4. The dots in Fig. 4 are placed on a cross-section of a polymeric composite and overlay a portion of one fibre and the matrix adjacent to it. The fibres are 5 μm in diameter, giving some indication of the very small size of the dots.

In principle, the dots produced in this way can be as small as the spot size of the beam. Beam spot size on the surface of a specimen depends on the type of filament used as well as the operating voltage and specimen current, as seen in Fig. 5 [9]. It is apparent from Fig. 5 that a beam size as small as 5 nm can be attained using a tungsten filament at 30 kV operating voltage. However, several factors, such as chromatic aberrations, instrument alignment and vibration, a.c. induced stray magnetic field interference, and specimen contamination may prevent the attainment of such a small spot size [9]. Furthermore, as the beam current becomes too small, the local heating rate is insufficient to produce a visible pucker.

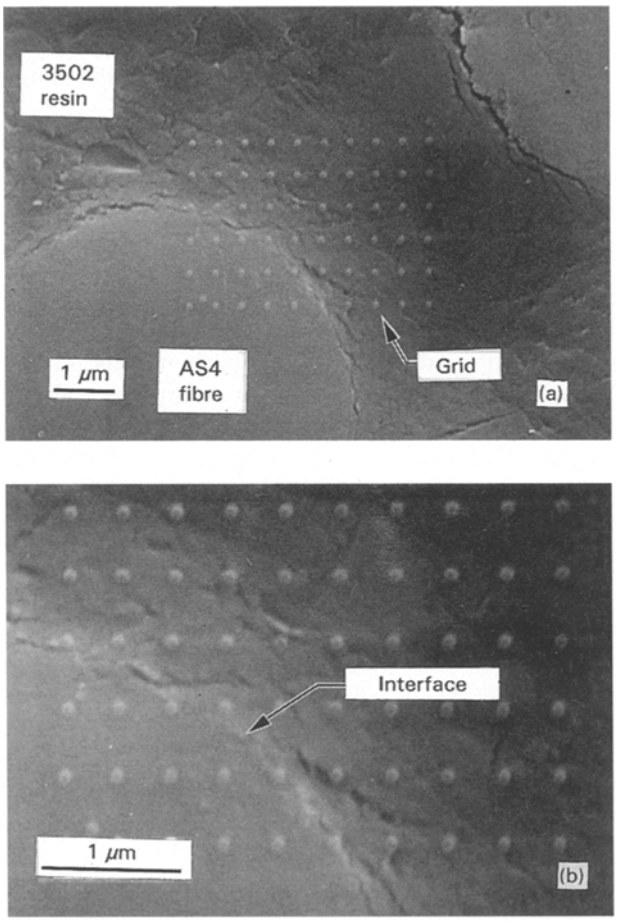

Figure 4 Cross-section of a graphite-epoxy composite on which fine dots have been placed by using the electron beam to heat surface contamination, giving a raised pucker. Note that these dots are much smaller than those produced by burning holes in the gold–palladium sputter coating.

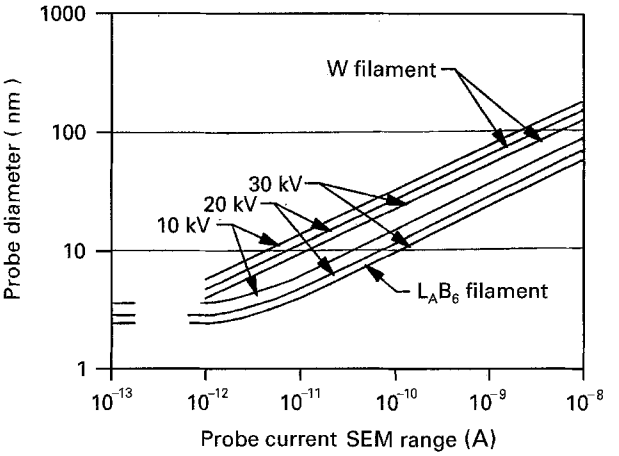

Figure 5 SEM beam spot size on specimen as a function of filament type, accelerating voltage and specimen current [9].

To determine the spot size achievable using contamination puckering, the accelerating voltage and specimen current in the SEM were varied systematically, with the results presented in Fig. 6 a, b. Both the total pucker diameter and the diameter of the black spot in the centre of the white pucker were measured. As expected, the highest accelerating voltage (30 kV) and the lowest specimen current capable of raising

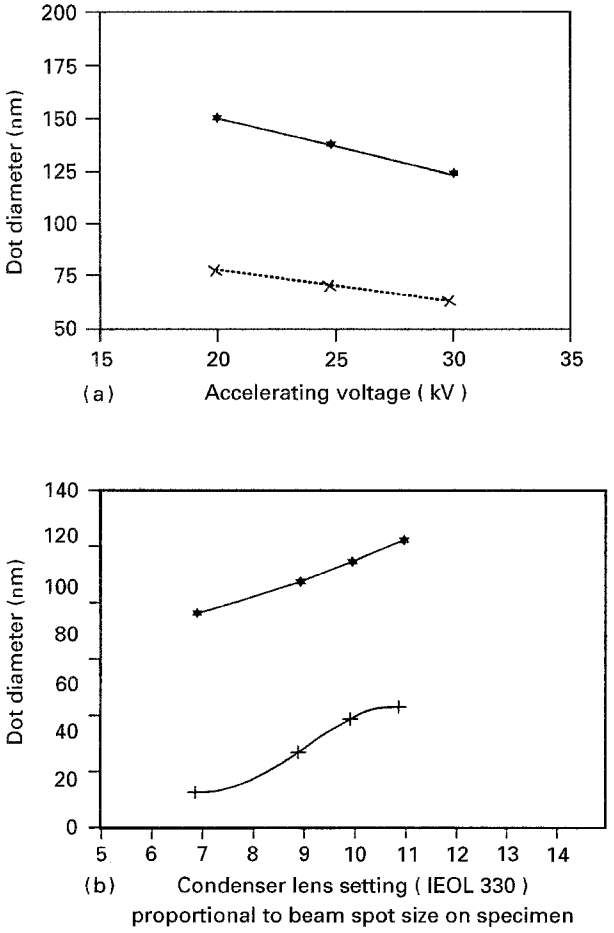

Figure 6 Variation in dot size produced as a function of (a) accelerating voltage for 10 s, and (b) specimen current at 30 kV for 10 s. (-✱-) outer dot diameter, (-×-) centre dot diameter.

puckers gave the finest spot size, which proved to be 90 nm, with a 30 nm black spot in the centre of the white dot. Such fine surface marking makes possible the study of strain fields on a very local scale, such as in the interphase region of a composite material.

3. Discussion

3.1. Illustrations of uses of the strain field mapping technique

The deformation which occurs in a laminated, polymeric composite has been studied using the dot mapping technique described in this paper. The dots which are produced by burning holes in the gold–palladium sputter coating were used for this work since the scale of the desired strain field map was approximately 100 μm, which is too large to be using dots which are less than 0.1 μm in diameter, such as those produced by puckering of surface contamination.

A unidirectional composite specimen of AS4 graphite fibres in an epoxy matrix of Hercules 3502 has been loaded in three point bending to give a nominally pure mode II state of stress at the delamination crack tip using a loading stage in the SEM. The SEM photograph is presented in Fig. 7a along with the resulting strain field map in Fig. 7b. Note the shear deformation is localized in the resin rich region between plies and reaches a maximum value of 20° rotation, which corresponds to $\varepsilon_{xy} = 0.175$. It is worth noting that this resin has a tensile test elongation of only 2%. While

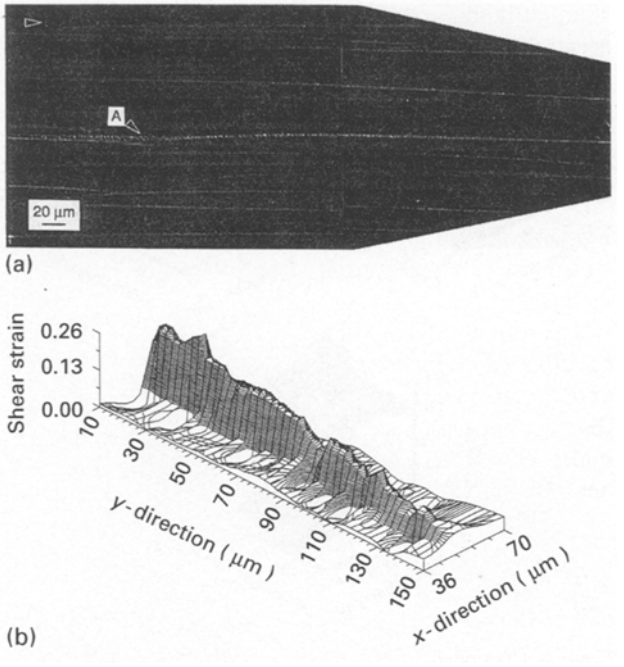

Figure 7 (a) Dot map of delamination crack growth under mode II loading in AS4/3502 unidirectional composite laminate and (b) strain field calculated from dot map.

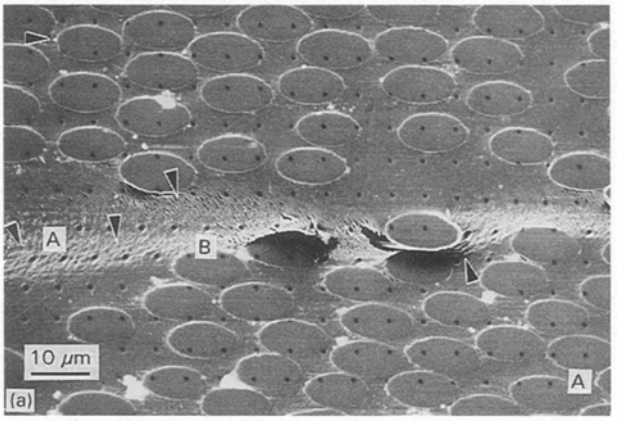

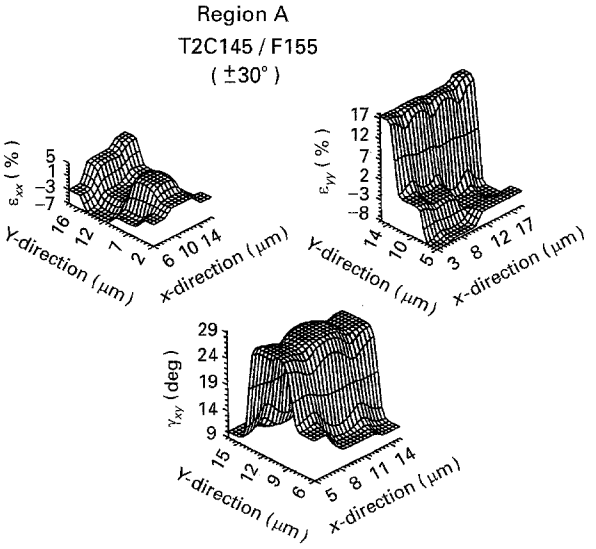

Figure 8 (a) Dot map of delamination crack growth under mode II loading in a T2C145/F155 composite laminate, with delamination occurring between ± 30° plies, and (b) strain field maps for locations labelled A and B in Fig. 7a.

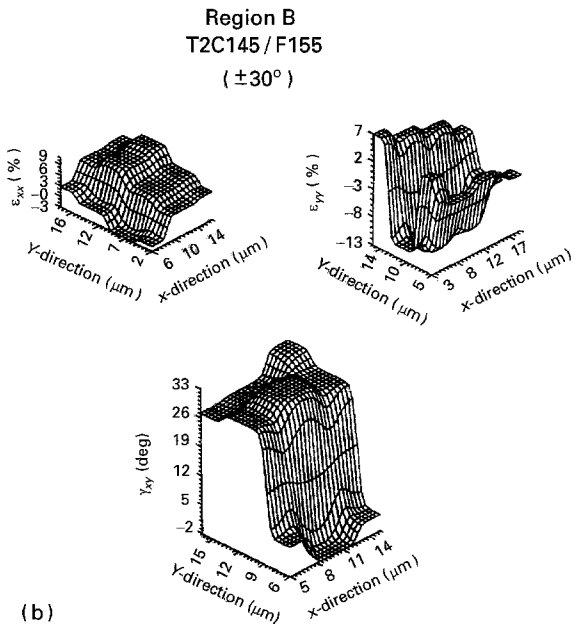

Figure 8 Continued

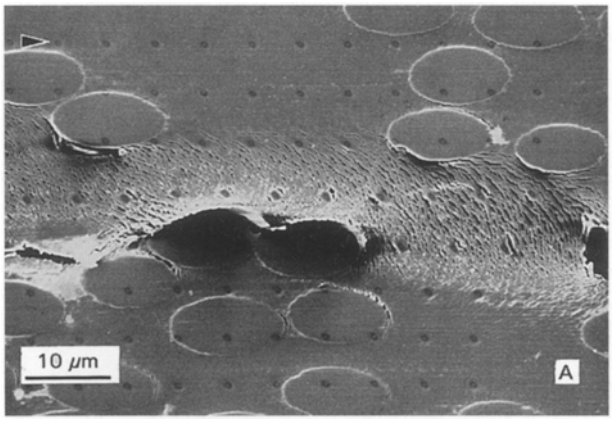

Figure 9 Additional photographs at high magnification of T2C145/F155 loaded to give mode II delamination crack growth between ± 30° plies. The very heterogeneous nature of the deformation is seen clearly qualitatively from the distortion of the dot map from its initial orthogonal grid.

a certain portion of the measured shear strain is in reality due to microcracking, a significant amount of it is due to resin deformation, again indicating the tensile elongation is controlled by incipient flaws rather than intrinsic ductility in epoxy resins.

A multidirectional composite (± 30°) composed of T2C145 graphite fibres in a matrix of rubber toughened epoxy (Hexcel F155) has also been deformed by loading it in three point bending in the SEM to give deformation under a nominally mode II state of stress. The results are presented in Fig. 8a, b. Note that high degree of heterogeneity in the deformation field, even in the resin rich region between plies. Fig. 9 shows additional photographs from this same specimen, indicating the ease with which the deformation field can be quantified using the dot map distortion. The deformation behaviour of the matrix is clearly facilitated in part by matrix cracking, though final failure seems to be initiated through interfacial failure. Dot mapping allows the critical strains for such events to be quantified.

Conclusions

Micrometre level strain field determination using dot mapping represents a powerful tool to study the deformation and fracture behaviour of materials at the microstructural scale.

Acknowledgements

This project was supported by the National Science Foundation, grant No. DMR9 017 530. The authors also wish to acknowledge the very professional assistance provided by the Electron Microscopy Center at Texas A&M University.

References

1. T. H. MAO, P. W. R. BEAUMONT, and W. C. NIXON, *J. Mater. Sci. Lett.* **2** (1983) 613.
2. N. BROWN and X. WANG *Polymer* **29** (1988) 463.
3. M. HIBBS and W. L. BRADLEY, Proceedings of Society of Experimental Mechanics Fall Meeting, October 1987, p. 87.
4. D. L. DAVIDSON and J. LANKFORD, *Int. J. Fracture* **17** (1981) 257.
5. M. R. JAMES, W. L. MORRIS, B. N. COX and M. S. DADKHAH, in "Micromechanics: Experimental Techniques", edited by W. N. Sharpe Jr. (American Society of Mechanical Engineers, New York, 1989) p. 89.
6. J. W. DALLY and D. T. READ, *Experimental Mech.* **33** (1993) 270.
7. D. POST, *ibid.* **31** (1991) 276.
8. W. N. SHARPE Jr, "Micromechanics: Experimental Techniques" (American Society of Mechanical Engineers, New York, 1989).
9. J. I. GOLDSTEIN, D. E. NEWBERRY, P. EHCIN, D. C. JOY, C. FIORI and E. LIFSHIN, "Scanning Electron Microscopy and X-Ray Microanalysis" (Plenum Press, New York, 1981), pp. 19–203.

Received 7 July 1994
and accepted 11 April 1995